

Estimating body volumes and surface areas of animals from cross-sections (#93869)

1

First submission

Guidance from your Editor

Please submit by **14 Jan 2024** for the benefit of the authors (and your token reward) .



Structure and Criteria

Please read the 'Structure and Criteria' page for general guidance.



Author notes

Have you read the author notes on the [guidance page](#)?



Raw data check

Review the raw data.



Image check

Check that figures and images have not been inappropriately manipulated.

If this article is published your review will be made public. You can choose whether to sign your review. If uploading a PDF please remove any identifiable information (if you want to remain anonymous).

Files

Download and review all files from the [materials page](#).

5 Figure file(s)

2 Latex file(s)

1 Raw data file(s)



Structure and Criteria

Structure your review

The review form is divided into 5 sections. Please consider these when composing your review:

1. **BASIC REPORTING**
2. **EXPERIMENTAL DESIGN**
3. **VALIDITY OF THE FINDINGS**
4. General comments
5. Confidential notes to the editor

 You can also annotate this PDF and upload it as part of your review

When ready [submit online](#).

Editorial Criteria

Use these criteria points to structure your review. The full detailed editorial criteria is on your [guidance page](#).

BASIC REPORTING

-  Clear, unambiguous, professional English language used throughout.
-  Intro & background to show context. Literature well referenced & relevant.
-  Structure conforms to [PeerJ standards](#), discipline norm, or improved for clarity.
-  Figures are relevant, high quality, well labelled & described.
-  Raw data supplied (see [PeerJ policy](#)).

EXPERIMENTAL DESIGN

-  Original primary research within [Scope of the journal](#).
-  Research question well defined, relevant & meaningful. It is stated how the research fills an identified knowledge gap.
-  Rigorous investigation performed to a high technical & ethical standard.
-  Methods described with sufficient detail & information to replicate.

VALIDITY OF THE FINDINGS

-  Impact and novelty not assessed. *Meaningful* replication encouraged where rationale & benefit to literature is clearly stated.
-  All underlying data have been provided; they are robust, statistically sound, & controlled.
-  Conclusions are well stated, linked to original research question & limited to supporting results.



The best reviewers use these techniques

Tip

Example

Support criticisms with evidence from the text or from other sources

Smith et al (J of Methodology, 2005, V3, pp 123) have shown that the analysis you use in Lines 241-250 is not the most appropriate for this situation. Please explain why you used this method.

Give specific suggestions on how to improve the manuscript

Your introduction needs more detail. I suggest that you improve the description at lines 57- 86 to provide more justification for your study (specifically, you should expand upon the knowledge gap being filled).

Comment on language and grammar issues

The English language should be improved to ensure that an international audience can clearly understand your text. Some examples where the language could be improved include lines 23, 77, 121, 128 – the current phrasing makes comprehension difficult. I suggest you have a colleague who is proficient in English and familiar with the subject matter review your manuscript, or contact a professional editing service.

Organize by importance of the issues, and number your points

1. Your most important issue
2. The next most important item
3. ...
4. The least important points

Please provide constructive criticism, and avoid personal opinions

I thank you for providing the raw data, however your supplemental files need more descriptive metadata identifiers to be useful to future readers. Although your results are compelling, the data analysis should be improved in the following ways: AA, BB, CC

Comment on strengths (as well as weaknesses) of the manuscript

I commend the authors for their extensive data set, compiled over many years of detailed fieldwork. In addition, the manuscript is clearly written in professional, unambiguous language. If there is a weakness, it is in the statistical analysis (as I have noted above) which should be improved upon before Acceptance.

Estimating body volumes and surface areas of animals from cross-sections

Ruizhe Jackevan Zhao ^{Corresp. 1}

¹ Department of Mathematics, Northwest University, Xi'an, China

Corresponding Author: Ruizhe Jackevan Zhao
Email address: JackevanChaos@outlook.com

Background: Body mass and surface area are among the most important biological properties, but such information is lacking for some extant organisms and all extinct species. Numerous methods have been developed for body size estimation of animals for this reason. There are two main categories of mass-estimating approaches: extant-scaling approaches and volumetric-density approaches. Extant-scaling approaches dig the relationships between linear skeletal measurements and body mass using regressions. Volumetric-density approaches, on the other hand, are all based on models. The models are of various types, including physical models, 2D images and 3D virtual reconstructions. After the models are established, their volumes are acquired using Archimedes' Principle, math formulas or 3D software. Then densities are designated to transform volumes into masses. Although often not emphasized, the acquisition of surface area is similar to mass estimation by changing math formulas or software commands. In this paper, a new 2D volumetric-density approach named cross-sectional method is presented. **Methods:** Cross-sectional method integrates biological cross-sections to obtain volume and surface area accurately. It requires a side view or dorsal/ventral view image, a series of cross-sectional silhouettes and some measurements to perform calculation. To evaluate the performance of cross-sectional method, two other 2D volumetric-density approaches (GDI and Paleomass) are compared with it. **Results:** Cross-sectional method generates very accurate results, with average error rates around 0.22% in volume and 1.18% in area respectively. It has higher accuracies than GDI or Paleomass when estimating the volumes and areas of irregular-shaped biological structures. **Discussion:** Most previous 2D volumetric-density approaches assume an elliptical or superelliptical approximation of animal cross-sections. Such an approximation does not always have good performances. Cross-sectional method processes the true profiles directly rather than approximating and can deal with any shapes. It can process objects which have gradually changing cross-sections. This study also suggests that more attention should be paid to careful acquisition of cross-sections of animals in 2D volumetric-density approaches, otherwise serious errors

might be generated during the estimations.

Estimating body volumes and surface areas of animals from cross-sections

Ruizhe Jackevan Zhao¹

¹Department of Mathematics, Northwest University, Xi'an, Shaanxi, China

Corresponding author:

Ruizhe Jackevan Zhao¹

Email address: jackevanchaos@outlook.com

ABSTRACT

Background: Body mass and surface area are among the most important biological properties, but such information is lacking for some extant organisms and all extinct species. Numerous methods have been developed for body size estimation of animals for this reason. There are two main categories of mass-estimating approaches: extant-scaling approaches and volumetric-density approaches. Extant-scaling approaches dig the relationships between linear skeletal measurements and body mass using regressions. Volumetric-density approaches, on the other hand, are all based on models. The models are of various types, including physical models, 2D images and 3D virtual reconstructions. After the models are established, their volumes are acquired using Archimedes' Principle, math formulas or 3D software. Then densities are designated to transform volumes into masses. Although often not emphasized, the acquisition of surface area is similar to mass estimation by changing math formulas or software commands. In this paper, a new 2D volumetric-density approach named cross-sectional method is presented.

Methods: Cross-sectional method integrates biological cross-sections to obtain volume and surface area accurately. It requires a side view or dorsal/ventral view image, a series of cross-sectional silhouettes and some measurements to perform calculation. To evaluate the performance of cross-sectional method, two other 2D volumetric-density approaches (GDI and Paleomass) are compared with it.

Results: Cross-sectional method generates very accurate results, with average error rates around 0.22% in volume and 1.18% in area respectively. It has higher accuracies than GDI or Paleomass when estimating the volumes and areas of irregular-shaped biological structures.

Discussion: Most previous 2D volumetric-density approaches assume an elliptical or superelliptical approximation of animal cross-sections. Such an approximation does not always have good performances. Cross-sectional method processes the true profiles directly rather than approximating and can deal with any shapes. It can process objects which have gradually changing cross-sections. This study also suggests that more attention should be paid to careful acquisition of cross-sections of animals in 2D volumetric-density approaches, otherwise serious errors might be generated during the estimations.

INTRODUCTION

Body mass and surface area are related to many biological properties such as physiology, ecology and evolution (Sato et al., 2006; McClain and Boyer, 2009; Benson et al., 2017; Kinoshita et al., 2021). Accurate estimations of these two values are often needed because unreliable results may lead to serious errors in subsequent researches (e.g., metabolic rate and speed calculation, Motani, 2002; Sato et al., 2009). However, body masses are unavailable for many large extant animals and all extinct organisms. Surface area information is also lacking because area can not be measured directly. To solve this problem, previous researchers have developed numerous approaches, most of which focused on body mass estimation.

In general, there are two categories of approaches for body mass estimation: extant-scaling approaches and volumetric-density approaches (Campione and Evans, 2020). Extant-scaling approaches utilize skeletal measurements as proxies and discover their relationships with body mass using regressions (Campbell et al., 1992; Campione et al., 2014). A classic and universally applied example of extant-scaling approaches is the equation for quadruped mass based on humeral and femoral circumference (Anderson et al., 1985).

The workflow of volumetric-density approaches is to create a reconstruction of the studied animal first, then its volume is obtained and an overall density is assigned to transform volume into mass (Hurlburt, 1999; Henderson, 1999; Motani, 2001). They have a much longer history than extant-scaling approaches, and numerous types of reconstructions have been developed over the past century, from physical models to 2D images to 3D virtual models. The earliest volumetric-density approaches are based on physical models. Gregory (1905) soaked a *Brontosaurus* model in water and acquired its volume using Archimedes' Principle, then he scaled the result to get the true value.

Some mathematical methods were developed later to calculate volume and surface area from 2D images. The first 2D volumetric-density method, Graphic Double Integration (GDI), was invented and introduced by Jerison (1969). Henderson (1999) developed a more rigorous math method called mathematical slicing to calculate volume and center of mass. Both GDI and mathematical slicing partition animals into several sections (known as "slabs" in Henderson, 1999) and treat them as frustums with elliptical bases. Seebacher (2001) invented a polynomial method, which uses polynomials and curve equations to simulate body outlines and cross-sections respectively. Motani (2001) argued that superellipses are better approximations of biological cross-sections rather than ellipses and developed the first version of Paleomass. The latest study on 2D volumetric-density approaches is the new version of Paleomass implemented in R (Motani, 2023).

With the rise of computer technology, three-dimensional modeling has been widely applied in animal reconstructions (Bates et al., 2009; Eriksson et al., 2022; Segre et al., 2023). The first step of 3D reconstruction of extinct vertebrates is to obtain the skeleton, which can be converted from photographs or 3D scans, then soft tissue is added to the skeleton. During this process, errors and subjectivity can not be avoided (Campione and Evans, 2020). Sellers et al. (2012) invented convex hull method, which generates minimum convex hulls to envelope the skeleton and adjusts the amount of soft tissue based on extant mammals. Convex hull method can reduce the errors introduced during soft tissue reconstructions, but it has the disadvantage that a large quantity of extant organisms are required as samples (Motani, 2023). After the reconstruction is accomplished, volume of the 3D model can be acquired instantly using software. Comparing with 2D approaches, three-dimensional modeling requires proficient use of 3D software and is more time-consuming, so there is still demand for developing 2D methods.

Although often ignored or not emphasized, surface areas can be obtained in a manner similar to acquiring volumes by changing math formulas in 2D approaches or applying different software commands in 3D approaches.

In this paper, a new 2D volumetric-density approach named cross-sectional method is presented. Cross-sectional method is a flexible approach that can handle any shape and can be applied to different animals from a wide stratigraphic range. It processes gradually changing cross-sections directly and produces estimations with high accuracies. Elliptical or superelliptical approximations of biological cross-sections, which are assumed in some other 2D volumetric-density approaches, are proved here to possess limited validity under certain conditions.

MATERIALS AND METHODS

Data Collection

To enable the calculation of body mass and surface area, some data are taken from the studied animal model (Fig. 1A). Protruding structures like flukes, limbs and horns are first separated from the main body (Fig. 1B). Their volumes and surface areas can be calculated independently using the same method applied in the main body part. Then the side view (or dorsal/ventral view) outline of the studied animal is collected by drawing along the profile from photos, precise life reconstructions or orthogonal projections of 3D models (Fig. 1C).

The terms "slab" and "subslab" used by Henderson (1999) are inherited here. After the outline is obtained, the animal's profile is equally partitioned into several slabs using parallel lines (Fig. 1D). The accuracy of the calculation increases together with the number of slabs. The portions of parallel lines truncated by the profile (i.e., maximum heights in side views or maximum widths in dorsal/ventral views) are defined here as "identity segments".

After partitioning, each slab (except the first and last one) can be regarded as a frustum with parallel bases, which are probably different in shape. The slabs at two ends of the animal's sagittal axis can be regarded as cones with irregular-shaped bases. In the humpback whale example shown in Figure 1, the tail fin is separated from the main body, hence only the anteriormost slab can be regarded as a cone. The

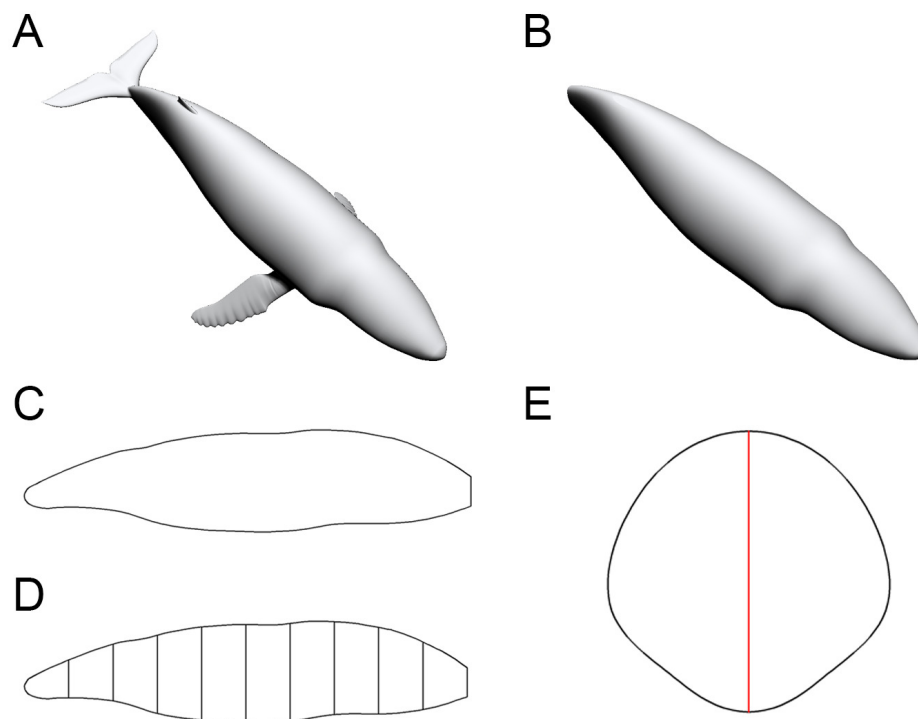


Figure 1. Data collection process of cross-sectional method. (A) 3D model of a humpback whale (*Megaptera novaeangliae*), from Gutarra et al. (2022). (B) Main body of the same model, with fins separated and removed. (C) Side view of the main body. (D) Side view of the main body after being sliced into 10 slabs. (E) One of the cross-sections of the main body, with identity segments marked in red.

102 next step is to collect the profiles of bases in each slab, which are originally body cross-sections of the
 103 studied animal (Fig. 1E). Then the area and circumference of each cross-section are acquired using image
 104 processing software.

105 **Body Volume Calculation**

Consider a slab having two parallel bases which are different in shape (Fig. 2A). Each base has an identity segment (denoted by d_0 and d_n respectively) as proxies for their areas (denoted by S_0 and S_n respectively). The ratio of S to d^2 is defined and denoted by φ , i.e.,

$$S = \varphi d^2$$

Then slice the slab equally into n subslabs with all the bases parallel to each other (n is a positive integer). Now consider an arbitrary subslab, say the k th one (Fig. 2B). The upper base and lower base of the k th subslab are indexed by B_{k-1} and B_k . The parameters (as defined above) of the lower base of the k th subslab are d_k , S_k , and φ_k respectively. Total height of the slab is denoted by L , and the height of each subslab is L_n . Assume that φ_k follows a linear relationship from φ_0 to φ_n , then

$$\varphi_k = k \left(\frac{\varphi_n - \varphi_0}{n} \right) + \varphi_0$$

Now consider the volume of the k th subslab. Length of identity segment d can not be simply assumed to increase or decrease linearly, because maximum body heights/widths along an animal's sagittal axis

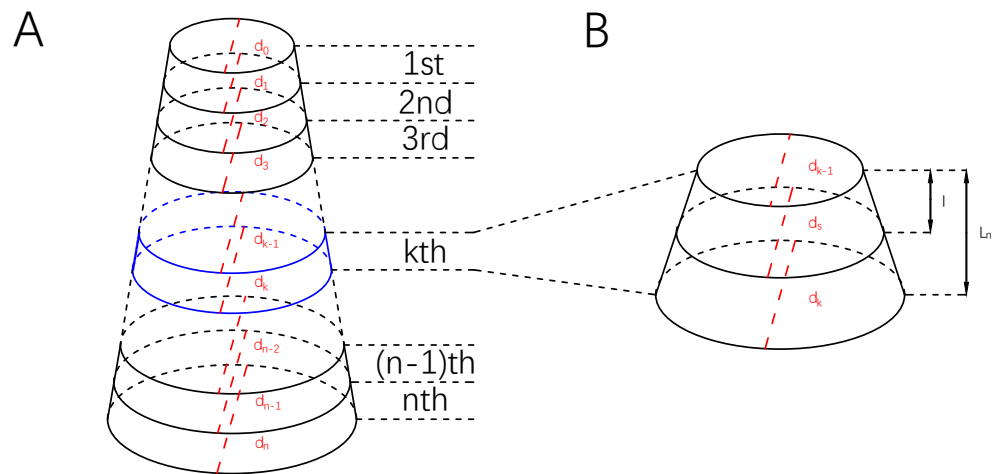


Figure 2. Illustrations of a slab and subslabs. (A) A slab equally partitioned into n subslabs, with identity segments marked in red and the k th subslab marked in blue. (B) The k th subslab and an arbitrary cross-section B_s , with identity segments marked in red.

often show irregular fluctuation. However, linearity is often used to approximate non-linearity at very small scales in calculus. If the partition of the slab is dense enough, it can be assumed that within each subslab d also follows a linear relationship. Then for any cross-section (denoted by B_s) in the k th subslab parallel to the bases B_{k-1} and B_k , it holds that

$$\varphi_s = \left(\frac{\varphi_k - \varphi_{k-1}}{L_n} \right) l + \varphi_{k-1}$$

$$d_s = \left(\frac{d_k - d_{k-1}}{L_n} \right) l + d_{k-1}$$

where l is the distance from B_s to B_{k-1} . Then let

$$\alpha_k = \frac{\varphi_k - \varphi_{k-1}}{L_n} \quad \beta_k = \frac{d_k - d_{k-1}}{L_n},$$

The area of cross-section B_s can be calculated by

$$\begin{aligned} S_s &= \varphi_s d_s^2 \\ &= (\alpha_k l + \varphi_{k-1})(\beta_k l + d_{k-1})^2 \\ &= \alpha_k \beta_k^2 l^3 + (2\alpha_k \beta_k d_{k-1} + \varphi_{k-1} \beta_k^2) l^2 \\ &\quad + (\alpha_k d_{k-1}^2 + 2\beta_k d_{k-1} \varphi_{k-1}) l + \varphi_{k-1} d_{k-1}^2 \end{aligned}$$

Then the volume of k th subslab is

$$\begin{aligned} V_k &= \int_0^{L_n} S_s dl \\ &= \frac{1}{4} \alpha_k \beta_k^2 L_n^4 + \frac{1}{3} (2\alpha_k \beta_k d_{k-1} + \varphi_{k-1} \beta_k^2) L_n^3 \\ &\quad + \frac{1}{2} (\alpha_k d_{k-1}^2 + 2\beta_k d_{k-1} \varphi_{k-1}) L_n^2 + \varphi_{k-1} d_{k-1}^2 L_n \end{aligned}$$

In particular, if φ is a constant (denoted by Φ), then $\alpha_k = 0$ and

$$V_k = \frac{1}{3}\Phi\beta_k^2L_n^3 + \beta_k d_{k-1}\Phi L_n^2 + \Phi d_{k-1}^2 L_n$$

The total volume of the slab is

$$V = \sum_{k=1}^n V_k$$

106 The two slabs at both ends of the animal's sagittal axis are processed as slabs with constant Φ if
107 they can be treated as cones, others are regarded to possess gradually changing cross-sections. The total
108 main body volume can be acquired by summing the volumes of all the slabs. The volumes of structures
109 separated (e.g., fins, limbs) from the main body are calculated using the same method.

110 Previous studies assigned distinct overall body densities to different animals (e.g., Henderson, 2006;
111 Larramendi et al., 2020), but a discussion of density variation among broad taxonomic clades is beyond
112 the scope of this study. In this paper, all animal models are treated as solid objects, with densities not
113 assigned (i.e., only the overall volumes are studied). Future scholars can easily acquire body masses by
114 assigning cavity sizes and densities to volumes calculated using the cross-sectional method.

115 Body Surface Area Calculation

Similar method is applied to calculate the surface area. All parameters defined in volume calculation except φ are inherited here. The circumferences of the upper base and lower base of the slab are denoted by C_0 and C_n . The ratio of C to d is denoted by ψ , i.e.,

$$C = \psi d$$

The parameters (as defined above) of the lower base of the k th subslab are d_k , C_k , and ψ_k . Assume that ψ_k follows a linear relationship from ψ_0 to ψ_n , then it holds that

$$\psi_k = k \left(\frac{\psi_n - \psi_0}{n} \right) + \psi_0$$

After slicing the slab equally into n subslabs, linearity is used to approximate non-linearity at very small scales:

$$\begin{aligned}\psi_s &= \left(\frac{\psi_k - \psi_{k-1}}{L_n} \right) l + \psi_{k-1} \\ d_s &= \left(\frac{d_k - d_{k-1}}{L_n} \right) l + d_{k-1}\end{aligned}$$

where l is the distance from B_s to B_{k-1} . Then let

$$\gamma_k = \frac{\psi_k - \psi_{k-1}}{L_n} \quad \beta_k = \frac{d_k - d_{k-1}}{L_n},$$

The circumference of cross-section B_s can be calculated by

$$\begin{aligned}C_s &= \psi_s d_s \\ &= (\gamma_k l + \psi_{k-1})(\beta_k l + d_{k-1}) \\ &= \gamma_k \beta_k l^2 + (\gamma_k d_{k-1} + \beta_k \psi_{k-1})l + \psi_{k-1} d_{k-1}\end{aligned}$$

Then the lateral surface area of k th subslab is

$$\begin{aligned}A_k &= \int_0^{L_n} C_s dl \\ &= \frac{1}{3}\gamma_k \beta_k L_n^3 + \frac{1}{2}(\gamma_k d_{k-1} + \beta_k \psi_{k-1})L_n^2 + \psi_{k-1} d_{k-1} L_n\end{aligned}$$

In particular, if ψ is a constant (denoted by Ψ), then $\gamma_k = 0$ and

$$A_k = \frac{1}{2}\beta_k \Psi L_n^2 + \Psi d_{k-1} L_n$$

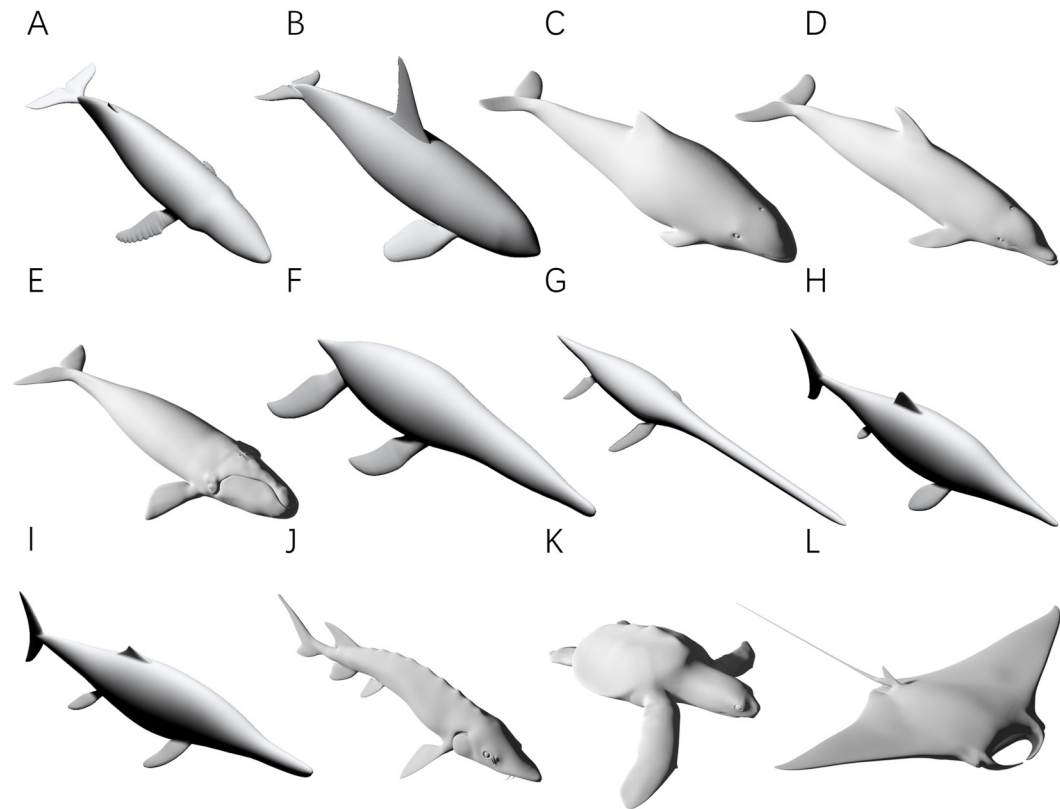


Figure 3. 3D models used for validation. (A) Humpback whale (*Megaptera novaeangliae*). (B) Orca (*Orcinus orca*). (C) Harbor porpoise (*Phocoena phocoena*). (D) Bottlenose dolphin (*Tursiops truncatus*). (E) Southern right whale (*Eubalaena australis*). (F) *Liopleurodon*. (G) *Thalassomedon*. (H) *Ophthalmosaurus*. (I) *Temnodontosaurus*. (J) Atlantic sturgeon (*Acipenser oxyrinchus oxyrinchus*). (K) Hawksbill sea turtle (*Eretmochelys imbricata*). (L) Manta ray (*Mobula c.f. birostris*). (A) (B) (F) (G) are from Gutarra et al. (2022), and (H) (I) are from Gutarra et al. (2019). Other models are produced by DigitalLife team in University of Massachusetts at Amherst (downloaded from <https://sketchfab.com/DigitalLife3D>, used with permission).

The total lateral surface area of the slab is

$$A = \sum_{k=1}^n A_k$$

116

117 The two slabs at both ends of the animal's sagittal axis are processed as slabs with constant Ψ if they
118 can be treated as cones, others are regarded to possess gradually changing cross-sections. The surface area
119 of the main body is calculated by summing the lateral areas of all slabs. The surface areas of structures
120 separated (e.g., fins, limbs) from the main body are calculated using the same method.

121 Validation and Comparison

122 To test the accuracy of cross-sectional method, three tests are carried out. In all three tests, the volumes
123 and surface areas of 3D models are first obtained, then the calculated results based on 2D methods are
124 compared with the true values to validate their accuracies. Only models precisely reproduced from
125 museum mounts, life photos or 3D scans are used for validation (see Gutarra et al., 2019, 2022, and
126 <http://digitallife3d.org/>). The models created by DigitalLife team contain some cavities for mouths and
127 gullets in their head regions, which may introduce extra errors affecting the evaluation of cross-sectional
128 method. Hence the heads of them are separated and not included in the tests. Each model is scaled to 1 m
129 in total length. To further evaluate the performances of cross-sectional method, GDI and Paleomass are

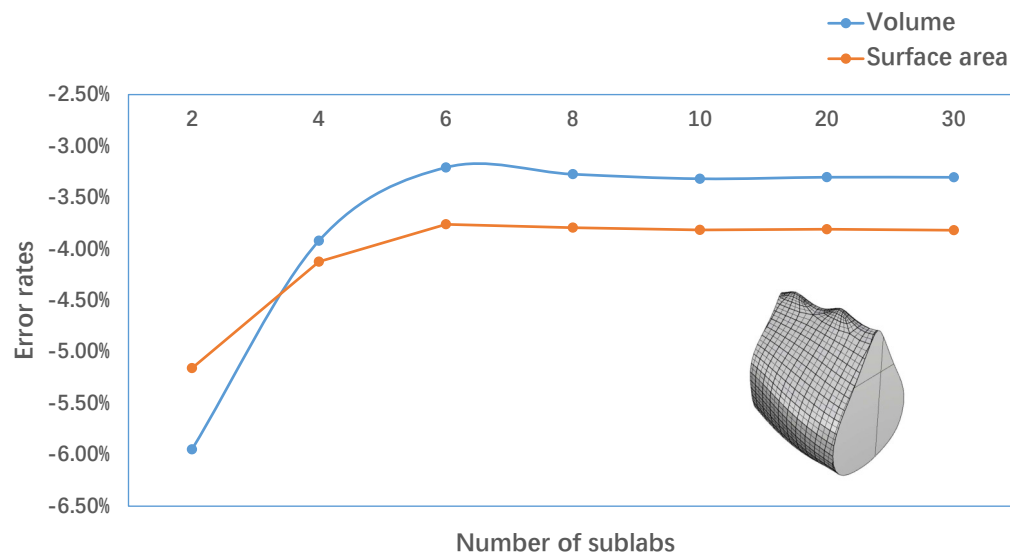


Figure 4. Results of the first test. The gray object is the slab tested, which is equally partitioned into 2, 4, 6, 8, 10, 20, 30 subslabs respectively. The blue curve is for error rates in volume and the orange one is for surface area.

included as representative methods for comparison, which approximate biological cross-sections with ellipses and superellipses respectively (Hurlburt, 1999; Motani, 2023). To ensure that the three methods can be compared in a same framework, twelve 3D models of extant or extinct aquatic animals are used (Fig. 3). Before the tests, protruding structures like limbs, flukes and fins are separated from the main body. Different structures from a same model may be used in different tests (see below).

The first test aims to reveal how many subslabs within a slab are required to produce relatively accurate volume and surface area estimations. A slab sliced from the Atlantic sturgeon model is used in this test (Fig. 4), which is partitioned into 2, 4, 6, 8, 10, 20, 30 subslabs respectively. Then calculation results are compared with the true values.

The second test aims to find out whether cross-sectional method has comparative or better performances than GDI or Paleomass when processing animals with near-circular cross-sections. The main bodies of five cetaceans, two plesiosaurs and two ichthyosaurs (Fig. 3A-I) are used in this test. The main body of each model has rounded or oval cross-sections, which can be well-approximated by ellipses or superellipses.

The third test aims to demonstrate that cross-sectional method still accurately estimates the volumes and surface areas when handling irregular-shaped biological structures. Models used in this test include fins and flippers of secondarily aquatic tetrapods (Fig. 3BFH), main body of an Atlantic sturgeon (Fig. 3F), main body of a hawksbill turtle (Fig. 3G) and pectoral fin of a manta ray (Fig. 3L).

Both the second and the third test compare the performances of cross-sectional method, GDI and Paleomass. Criteria applied in these two tests are described below. In GDI, each object is first equally sliced into 10 slabs, then the volume is calculated using the formula proposed by Hurlburt (1999) after necessary measurements are made. Paleomass is performed using the corresponding package in R (Motani, 2023). The four fin examples in the third test are treated as foils and others are treated as main bodies (for detailed methods, see Motani, 2023). k-value range is set to 2-2.3 in the second test. This is the range suitable for modern cetaceans (Motani, 2023), and it is assumed that the k-values of plesiosaurs and ichthyosaurs also fall in this range. In the third test, k-value range is set to 1.6-2.4, which successfully brackets all aquatic species tested by Motani (2023). To enable the calculation of error rates and comparison with other methods, average value of the upper bound and lower bound provided by Paleomass is calculated for each model, following Motani (2023). In cross-sectional method, each object is equally sliced into 10 slabs and each slab is further partitioned into 10 subslabs, then the volume and surface area are calculated after parameters of the bases in each subslab are obtained.

Table 1. Error rates in the second test. CS is short for cross-sectional method. Models that aren't bracketed by Paleomass are marked in red.

Model	Volume			Surface Area		
	GDI	Paleomass	CS	GDI	Paleomass	CS
Humpback whale	1.81%	6.77%	0.25%	-1.65%	6.25%	-1.52%
Orca	-2.88%	2.05%	-0.16%	-0.44%	3.56%	0.79%
Harbor porpoise	0.07%	2.50%	-0.35%	-1.06%	0.02%	-0.89%
Bottlenose dolphin	1.97%	3.31%	0.12%	-0.36%	1.01%	-0.59%
Southern right whale	6.01%	7.90%	-0.06%	1.67%	2.92%	-1.24%
<i>Liopleurodon</i>	-0.16%	5.33%	-0.02%	-2.81%	2.46%	-1.94%
<i>Thalassomedon</i>	-5.53%	0.91%	-0.17%	-4.34%	0.38%	-0.53%
<i>Ophthalmosaurus</i>	-3.90%	0.64%	0.15%	-3.28%	0.31%	-2.04%
<i>Temnodontosaurus</i>	-2.46%	2.02%	0.12%	-2.70%	1.04%	-0.75%
Mean	2.75%	3.49%	0.16%	2.03%	1.99%	1.14%

After calculation, the error rates generated by different methods are compared. Error rate is defined as

$$\text{Error Rate} = \frac{\text{Calculated Value} - \text{True Value}}{\text{True Value}}$$

when the calculation underestimates the true value, the error rate is negative; when overestimating, the error rate is positive. Afterwards the mean error is calculated as:

$$\text{Mean Error} = \frac{\sum |\text{Error Rate}|}{\text{Sample Number}}$$

Software Application

All the 3D models are first processed in Rhino 7. Each model is separated using *WireCut* command, then the volume and surface area of the selected part are acquired using *Volume* and *Area* command respectively. Side view and dorsal/ventral view images of the separated models are obtained with *Make2D* command. To generate the cross-sections needed in cross-sectional method, *ClippingPlane* command is used.

Two dimensional images are then imported into AutoCAD 2020, where they are sliced into slabs or subslabs using *Arrayrect* and *Trim* commands. Measurements of each slab or subslab are taken and exported into Excel with *Dataextraction* command. In cross-sectional method, areas, circumferences and lengths of identity segments of the bases in each subslab are first measured with *Measuregeom* command, then the parameters ϕ and ψ are calculated with the calculator implemented in AutoCAD. The calculation of GDI and cross-sectional method is finally performed in Excel.

Both Rhino and AutoCAD are industrial software with a high precision. They have already been applied in previous studies for body size estimation of extinct animals and proved to have good performances (e.g., Henderson, 1999; McHenry, 2009).

Paleomass implemented in R requires bitmaps (Motani, 2023), so the two-dimensional images are exported from AutoCAD as PNGs. Each PNG is set to possess 6000×4000 pixels since Motani (2023) suggested that Paleomass has better performances when handling images with higher resolution. They are then imported into PhotoShop 2020 for dyeing. Afterwards the processed images are imported into R 4.1.3, where the final calculation takes place.

RESULTS

Error rates of the three tests are presented in Figure 4, Table 1 and Table 2 respectively. The detailed results can be found in supplementary material.

Figure 4 shows the results of the first test. It demonstrates that the error rates tend to stabilize for both volume and area estimations when the number of subslabs increases to 10 or more. It is notable that the error rates are relatively high when stabilized (around -3.30% in volume and -3.82 % in area), but this is not related to the number of subslabs. The slab occupies a large portion of main body of the Atlantic

Table 2. Error rates in the third test. CS is short for cross-sectional method. Models that aren't bracketed by Paleomass are marked in red.

Model	Volume			Surface Area		
	GDI	Paleomass	CS	GDI	Paleomass	CS
<i>Liopleurodon</i> flipper	14.29%	24.16%	−0.25%	6.22%	4.30%	−0.06%
Orca dorsal fin	12.92%	−29.55%	−0.27%	7.66%	−12.94%	−1.10%
<i>Ophthalmosaurus</i> tail fin	12.25%	15.44%	−0.42%	6.18%	0.74%	−1.40%
Manta ray pectoral fin	16.68%	−57.32%	−0.48%	6.26%	−12.38%	−1.93%
Atlantic sturgeon main body	12.51%	9.84%	−0.28%	−0.88%	5.88%	−1.49%
Hawksbill turtle main body	17.46%	14.43%	0.10%	4.85%	8.06%	−1.38%
Mean	14.35%	25.12%	0.30%	5.34%	7.39%	1.22%

sturgeon model, and the accuracy of cross-sectional method can be improved by dividing it into more slabs (i.e., obtaining more thoracic cross-sections), as shown in the third test.

Table 1 shows the results of the second test, models that aren't bracketed by Paleomass are marked in red. All the three methods validated show good performances, with error rates lower than 5% than by average. This corroborates the validity of 2D volumetric-density methods when handling animals with rounded or oval cross-sections, as demonstrated in previous studies (Henderson, 1999; Motani, 2023). In both volume and surface area calculation, cross-sectional method shows slightly higher accuracies than GDI and Paleomass.

In the third test, the error rates of GDI and Paleomass increase significantly (Table 2). This indicates that an elliptical approximation, as assumed in GDI, is not suitable for all biological cross-sections. Paleomass treats the four fin/flipper samples as foils, which are described by an equation with one variable controlling for relative thickness (t-value, see Motani, 2023). However, high error rates occur in the estimated results from Paleomass in these samples. Paleomass also fails to bracket the true values of the Atlantic sturgeon and hawksbill turtle with the selected range of k-values (1.6-2.4). Cross-sectional method generally has much better performances than GDI or Paleomass in the third test, with error rates always lower than 2%.

DISCUSSION

The rationale for including extinct animals in the tests merits a discussion. The body outlines of most extinct animals are unknown, and the 3D models remain interpretive reconstructions. But body volumes and surface areas are always obtained after the models are established in all volumetric-density methods. In another word, all volumetric-density methods actually estimate the volumes and surface areas of the models rather than true animals. The inclusion of extinct animals in the tests successfully proves that cross-sectional method can provide accurate volume and area estimations of artificial models which are based on fossils. Thus it is a flexible method that can be applied to different animal models from a large stratigraphic range. On the other hand, the error rates of Paleomass on these extinct animal models bear limited reference value because the workflow of Paleomass in R includes using images to generate 3D models, which may be distinct from the original ones.

The purpose behind the comparison of the three methods is to demonstrate the limitation of elliptical or superelliptical approximation. It has been long assumed that the cross-sections of an animal's main body or limbs can be approximated by ellipses (Campione and Evans, 2020). Based on this assumption some mathematical methods were developed to calculate the volumes and surface areas of animals from 2D images (e.g., GDI, Jerison, 1969; mathematical slicing, Henderson, 1999). In some species with rounded or oval cross-sections, elliptical approximation does have good performances, as proved in the second test (Table 1).

In GDI, the semi-major and semi-minor axes of the bases in each slab are measured, then the average values are taken and the slab is treated as a cylinder with elliptical cross-sections (for detailed formula, see Hurlburt, 1999). This assumption is not mathematically rigorous, but it proves to have high accuracies (>95%) when handling objects with near elliptical cross-sections (Jerison, 1969). But error rates increase to more than 10% when evaluating irregular-shaped objects in the third test, revealing the limited validity of this method under certain conditions.

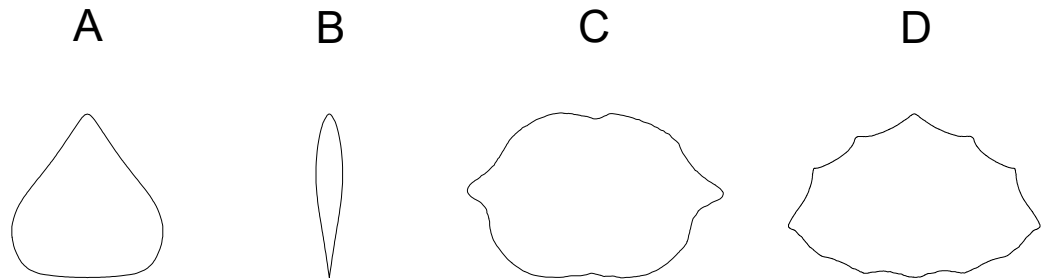


Figure 5. Irregular biological cross-sections. (A) Body cross-section of an Atlantic sturgeon (*Acipenser oxyrinchus oxyrinchus*); (B) Cross-section of flipper/fin of secondarily aquatic tetrapods, reproduced from Gutarra and Rahman (2021); (C) Body cross-section of a Japanese giant salamander (*Andrias japonicus*); (D) Body cross-sections of a leatherback turtle (*Dermochelys coriacea*). (A)(C)(D) are truncated from accurate 3D models produced by DigitalLife team within University of Massachusetts at Amherst (downloaded from <https://sketchfab.com/DigitalLife3D> and used with permission).

Motani (2001) noticed that some cross-sections in nature can not be well represented by ellipses. This is supported by the Atlantic sturgeon model, which has almost triangular thoracic cross-sections (Fig. 5A). There are many irregular-shaped cross-sections in nature. It is not possible to list all of them in this paper, but some are presented here as examples: (1) The cross-sections of fins and limbs in lift-based underwater fliers (e.g., plesiosaurs) and axial swimming tetrapods (e.g., ichthyosaurs and cetaceans) are hydrodynamic foils (Fig. 5B, Robinson, 1975; Gutarra and Rahman, 2021). (2) Giant salamanders have folds of skin along their body flanks, leading to irregular-shaped cross-sections (Fig. 5C). (3) Leatherback turtles have rugose shells with multiple ridges (Fig. 5D). Due to the presence of such objects, Motani (2001) developed Paleomass, which produces intervals to bracket the true volumes and areas using superellipses. The formula describing a superellipse is

$$\left| \frac{x}{a} \right|^k + \left| \frac{y}{b} \right|^k = 1$$

where a and b are semi-major and semi-minor axes respectively. It is notable that this formula represents an ellipse when k equals 2. Although Paleomass has good performances when bracketing animals with suitable k -values, point estimations are normally required in subsequent researches (e.g., kinematic analysis, Sato et al., 2006). Taking the average values of intervals may be an option, but it can not be guaranteed that the true values are always close to the average values. It is demonstrated in the second test that taking the average values may lead to higher error rates than GDI even though the true values are bracketed successfully (Table 1). In addition, taking a point estimation is identical to approximate cross-sections using superellipses with a constant k -value.

In the second test, Paleomass shows good performances in handling the main bodies of aquatic tetrapods, with 3.49 % error rates in volume and 1.99% in area by average. This proves the effectiveness of superelliptical bracketing in animals which have barrel-shaped bodies. However, Paleomass fails to bracket the true values of the humpback whale and the southern right whale, leading to higher error rates than in other cetaceans. It is notable that the selected k -value range 2-2.3 is summarized from only two samples (*Phocoena phocoena* and *Tursiops truncatus*) and they occupy the upper bound and lower bound of this interval respectively (Motani, 2023). Thus maybe more samples are needed to clarify the true k -value range for all cetaceans.

Paleomass generates significant errors when estimating the values of the flipper/fin examples in the third test. It is possible that a single formula with only one variable controlling for thickness may not be sufficient to describe all types of fins and flippers. Paleomass also fails to bracket the Atlantic sturgeon and hawksbill turtle using k -value range 1.6-2.4, possibly due to the irregular cross-sections of them. The accuracy of Paleomass on these two models can be improved by selecting more suitable k -values, but this reveals another problem: it is not known which k -value range to use when handling animal clades that have not been examined before. This problem is especially tricky for most extinct animals, as their true

body cross-sections are unavailable.

The cross-sectional method presented in this paper calculates volumes and surface areas from cross-sectional profiles directly rather than approximating. Instead of testing the performances of cross-sectional method on complete models, irregular-shaped biological structures are separated and tested independently. This is because such structures (e.g. fins in aquatic animals) are sometimes so small that errors in them hardly make significant impacts on total accuracies. Although all examples tested are aquatic species, cross-sectional method can also process terrestrial or flying animals if the models are appropriately separated and partitioned. Results of the first test suggest that the error rates in estimating the volume and area of a slab will tend to stabilize with the increase in number of subslabs. The accuracy of cross-sectional method in such cases can be improved by dividing the models into more slabs and obtaining more cross-sections.

In the second and third test, each model is sliced into 10 slabs and each slab is further partitioned into 10 subslabs. Under this criterion, cross-sectional method generates more accurate estimations for volumes and areas than GDI or Paleomass. Processing profile images may incorporate extra errors, but the total error rates are around or lower than 2% in all cases tested. Unlike many previous 2D volumetric-density approaches which assume a constant superelliptical k-value ($k=2$ for ellipse) along the sagittal axis, this method is more flexible by assuming and handling gradually changing cross-sections. It generates point estimation results rather than interval estimations, hence the results can be directly incorporated in following studies like scaling regressions (see “hybrid approaches” in Campione and Evans, 2020).

The disadvantage of cross-sectional method is that it requires a series of cross-sectional profiles, which is often unavailable because it didn't receive enough attention. Cross-sectional outlines can be extracted from front view photos, dissections, 3D scans or precise reconstructions. Paul (2022) suggested that accurate skeleton profiles are essential to reconstruct extinct or extant vertebrates, but a rigorous reconstruction of the rib cage is often ignored or not published in previous studies. Careful examination of cross-sections is, however, also suggested in previous studies (e.g., Motani, 2001). I suggest future scholars pay more attention to detailed and careful reconstruction or acquisition of cross-sectional profiles because simply assuming an elliptical or superelliptical cross-section may lead to serious errors, as proved in this paper.

CONCLUSION

Cross-sectional method is a new 2D volumetric-density approach, which processes cross-sectional profiles directly rather than approximating. Cross-sectional method requires a side view or dorsal/ventral view image and a series of cross-sectional silhouettes to perform calculation. It integrates biological cross-sections into volumes and surface areas and produces point estimations. Cross-sectional method generates results with a high accuracy, with average error rates around 0.22% in volume and 1.18% in area. Instead of assuming elliptical or superelliptical cross-sections empirically, future scholars are suggested to carefully examine the profiles to acquire the true shapes.

ACKNOWLEDGEMENT

I thank Beneden Parotodus for assessing math formulas before publication. Andrew Orkney is thanked for advice on improving the manuscript.

REFERENCES

- Anderson, J. F., Hall-Martin, A., and Russell, D. A. (1985). Long-bone circumference and weight in mammals, birds and dinosaurs. *Journal of Zoology*, 207(1):53–61.
- Bates, K. T., Manning, P. L., Hodgetts, D., and Sellers, W. I. (2009). Estimating mass properties of dinosaurs using laser imaging and 3d computer modelling. *PloS one*, 4(2):e4532.
- Benson, R. B. J., Hunt, G., Carrano, M. T., and Campione, N. (2017). Cope's rule and the adaptive landscape of dinosaur body size evolution. *Palaeontology*, 61(1):13–48.
- Campbell, K. E., Marcus, L., et al. (1992). The relationship of hindlimb bone dimensions to body weight in birds. *Natural History Museum of Los Angeles County Science Series*, 36(3):395–412.
- Campione, N. E. and Evans, D. C. (2020). The accuracy and precision of body mass estimation in non-avian dinosaurs. *Biological Reviews*, 95(6):1759–1797.

- 301 Campione, N. E., Evans, D. C., Brown, C. M., and Carrano, M. T. (2014). Body mass estimation in
302 non-avian bipeds using a theoretical conversion to quadruped stylopodial proportions. *Methods in*
303 *Ecology and Evolution*, 5(9):913–923.
- 304 Eriksson, M. E., Garza, R. D. L., Horn, E., and Lindgren, J. (2022). A review of ichthyosaur (rep-
305 tilia, ichthyopterygia) soft tissues with implications for life reconstructions. *Earth-Science Reviews*,
306 226:103965.
- 307 Gregory, W. (1905). The weight of the *Brontosaurus*. *Science*, 22(566):572–572.
- 308 Gutarra, S., Moon, B. C., Rahman, I. A., Palmer, C., Lautenschlager, S., Brimacombe, A. J., and
309 Benton, M. J. (2019). Effects of body plan evolution on the hydrodynamic drag and energy re-
310 quirements of swimming in ichthyosaurs. *Proceedings of the Royal Society B: Biological Sciences*,
311 286(1898):20182786.
- 312 Gutarra, S. and Rahman, I. A. (2021). The locomotion of extinct secondarily aquatic tetrapods. *Biological*
313 *Reviews*, 97(1):67–98.
- 314 Gutarra, S., Stubbs, T. L., Moon, B. C., Palmer, C., and Benton, M. J. (2022). Large size in aquatic
315 tetrapods compensates for high drag caused by extreme body proportions. *Communications Biology*,
316 5(1).
- 317 Henderson, D. M. (1999). Estimating the masses and centers of mass of extinct animals by 3-d mathemat-
318 ical slicing. *Paleobiology*, 25(1):88–106.
- 319 Henderson, D. M. (2006). Floating point: a computational study of buoyancy, equilibrium, and gastroliths
320 in plesiosaurs. *Lethaia*, 39(3):227–244.
- 321 Hurlburt, G. (1999). Comparison of body mass estimation techniques, using recent reptiles and the
322 pelycosaur *Edaphosaurus boanerges*. *Journal of Vertebrate Paleontology*, 19(2):338–350.
- 323 Jerison, H. J. (1969). Brain evolution and dinosaur brains. *The American Naturalist*, 103(934):575–588.
- 324 Kinoshita, C., Fukuoka, T., Narazaki, T., Niizuma, Y., and Sato, K. (2021). Analysis of why sea turtles
325 swim slowly: a metabolic and mechanical approach. *Journal of Experimental Biology*, 224(4).
- 326 Larramendi, A., Paul, G. S., and Yu Hsu, S. (2020). A review and reappraisal of the specific gravities
327 of present and past multicellular organisms, with an emphasis on tetrapods. *The Anatomical Record*,
328 304(9):1833–1888.
- 329 McClain, C. R. and Boyer, A. G. (2009). Biodiversity and body size are linked across metazoans.
330 *Proceedings of the Royal Society B: Biological Sciences*, 276(1665):2209–2215.
- 331 McHenry, C. R. (2009). *Devourer of gods: the palaeoecology of the Cretaceous pliosaur Kronosaurus*
332 *queenslandicus*. PhD thesis, University of Newcastle.
- 333 Motani, R. (2001). Estimating body mass from silhouettes: testing the assumption of elliptical body
334 cross-sections. *Paleobiology*, 27(4):735–750.
- 335 Motani, R. (2002). Swimming speed estimation of extinct marine reptiles: energetic approach revisited.
336 *Paleobiology*, 28(2):251–262.
- 337 Motani, R. (2023). Paleomass for r—bracketing body volume of marine vertebrates with 3d models.
338 *PeerJ*, 11:e15957.
- 339 Paul, G. S. (2022). Restoring the true form of the gigantic blue whale for the first time, and mass
340 estimation. *BioRxiv*, pages 2022–08.
- 341 Robinson, J. A. (1975). The locomotion of plesiosaurs. *Neues Jahrbuch für Geologie und Paläontologie*,
342 *Abhandlungen*.
- 343 Sato, K., Shiomi, K., Watanabe, Y., Watanuki, Y., Takahashi, A., and Ponganis, P. J. (2009). Scaling of
344 swim speed and stroke frequency in geometrically similar penguins: they swim optimally to minimize
345 cost of transport. *Proceedings of the Royal Society B: Biological Sciences*, 277(1682):707–714.
- 346 Sato, K., Watanuki, Y., Takahashi, A., Miller, P. J., Tanaka, H., Kawabe, R., Ponganis, P. J., Handrich,
347 Y., Akamatsu, T., Watanabe, Y., Mitani, Y., Costa, D. P., Bost, C.-A., Aoki, K., Amano, M., Trathan,
348 P., Shapiro, A., and Naito, Y. (2006). Stroke frequency, but not swimming speed, is related to body
349 size in free-ranging seabirds, pinnipeds and cetaceans. *Proceedings of the Royal Society B: Biological*
350 *Sciences*, 274(1609):471–477.
- 351 Seebacher, F. (2001). A new method to calculate allometric length-mass relationships of dinosaurs.
352 *Journal of vertebrate Paleontology*, 21(1):51–60.
- 353 Segre, P. S., Martin, J., Irschick, D. J., and Goldbogen, J. A. (2023). A three-dimensional, dynamic blue
354 whale model for research and scientific communication. *Marine Mammal Science*, 39(3):1011–1018.
- 355 Sellers, W. I., Hepworth-Bell, J., Falkingham, P. L., Bates, K. T., Brassey, C. A., Egerton, V. M., and

356 Manning, P. L. (2012). Minimum convex hull mass estimations of complete mounted skeletons. *Biology*
 357 *Letters*, 8(5):842–845.

Basic Reporting

The use of English is almost fine. I have revised some of the word usage and phrases. In many places the definite article 'the' is needed.

The introduction and background information are almost fine. The introduction does a good job of reviewing previous mass estimation methods, but fails on prior surface area estimations. This is unfortunate as the method proposed in the paper does make and test surface area estimates. Two examples of the applications of animal surface area estimates can be found in these two papers:

Henderson, D. M. (2013). "Sauropod necks: were they really for heat loss?" *PLoS ONE* **8**(10): 1-8.

Sereno, P. C., et al. (2022). "Spinosaurus is not an aquatic dinosaur." *eLife* **2022**: 1-15. (Figure 5)

The figures are almost fine. The dashed diagonals representing the diameters on figure 2 are confusing and took me a few seconds to realize what they were trying to show, and should be drawn differently. Also, the representative frustum and its subsection should be shown with same orientation as the body forms shown in figures 1 and 3.

Several sets of cross-sections from the full axial bodies and limbs from a limited selection of the models shown in figure 3 should be presented. The samples should include one each of a toothed and baleen cetacean, an ichthyosaur, a plesiosaur, the sturgeon and the turtle.

Experimental Design

The research is appropriate for PeerJ. As the author states in the text, knowing the body masses for animals provides a foundation for other studies. The new cross-sectional method is described in sufficient detail to enable replication, and does produce valid results, and the testing and comparison of this new method appears to be adequate.

Validity of the Findings

The results are reasonable. The conclusions are supported by the presented data.

General Comments

At first glance the method does simpler and more direct, but the complexity of generating the initial 3D models that are used for the sources of the contours is glossed over. It appears that the Rhino software used to produce the models already generates volumes and surface areas, so the new method seems a bit redundant.

The author has missed an opportunity to compute the centroid of the 3D shapes being analyzed. By adding an extra 'l' term in the integrand at the bottom of page 4, the centroid, \bar{l} , for the k^{th} body segment could be determined with the following expression:

$$\bar{l} = \frac{\int_0^{L_n} S_s dl}{\int_0^{L_n} S_s dl}$$

This could be extended to determine the centroid for an entire body region. The centroid is useful to locating the balance point (if a density distribution is developed) or the centre of pressure for lift calculations (eg. for the underwater flying manta ray).

One serious limitation of the method is that it appears to depend on the body or body part being straight. Curved structures such as necks or tails would confound the simple, linear scaling used. I would like to see if this new method could cope with the curved neck of a sauropod. See that attached image of a sauropod that could be used to test this. This image is from Henderson (2013) cited above.

The author presents the method, but it is up to the motivated reader to implement it. Most of the biologists and palaeontologists that I know could not even begin to develop the software to implement the method. Motani (2023), the author whose method is criticized by the present author, does make his software available for use.

